HHS Public Access

Author manuscript

Int J Radiat Oncol Biol Phys. Author manuscript; available in PMC 2023 February 01.

Published in final edited form as:

Int J Radiat Oncol Biol Phys. 2022 February 01; 112(2): 475–486. doi:10.1016/j.ijrobp.2021.09.010.

Boosting the abscopal effect using immunogenic biomaterials with varying radiotherapy field sizes

Sayeda Yasmin-Karim, PhD[1,*], **Bashkim Ziberi, PhD**[2,3], **Johanna Wirtz, MD**[2,4], **Noella Bih, BS**[1], **Michele Moreau, MS**[1,5], **Romy Mueller, PhD**[1,6], **Victoria Anisworth, MS**[2,5], **Juergen Hesser, PhD**[6], **G. Mike Makrigiorgos, PhD**[1], **Michael D Chuong, MD**[7], **Xiao Xiao Wei, MD**[1], **Paul L. Nguyen, MD**[1,**], **Wilfred Ngwa, PhD**[1,5,**]

[1]Dana Farber Cancer Institute, Brigham and Women's Hospital, Harvard Medical School, Boston, Massachusetts, USA

[2]Dana Farber Cancer Institute, Harvard Medical School, Boston, Massachusetts, USA

[3]University of Tetova, Tetova, Republic of North Macedonia

[4]Medical Faculty of University Ulm, Ulm, Germany

[5]University of Massachusetts, Lowell, Massachusetts, USA

[6]Data Analysis and Modeling in Medicine, Mannheim Institute for Intelligent Systems in Medicine (MIISM), Heidelberg University, 69117 Heidelberg, Germany

[7]Miami Cancer Institute, Baptist Health South Florida, Miami, Florida, USA.

Abstract

Purpose: Persistent immunosuppression in the tumor micro-environment is a major limitation to boosting the abscopal effect, whereby radiotherapy at one site can lead to regression of tumors at distant sites. Here, we investigate the use of radiation and immunogenic biomaterials (IBM) targeting only the gross tumor sub-volume for boosting the abscopal effect in immunologically cold tumors.

Methods: To evaluate the abscopal effect, two syngeneic contralateral tumors were implanted in each mouse, where only one tumor was treated. IBM was administered to the treated tumor with one fraction of radiation and results were compared, including as a function of different radiotherapy field sizes. The IBM was designed similar to fiducial markers using immunogenic

[*]**Corresponding author:** Name: Sayeda Yasmin-Karim, sayeda_yasmin-karim@dfci.harvard.edu (S.Y.).
[**]Co-senior authors
Author Responsible for Statistical Analysis:
Sayeda Yasmin-Karim [Sayeda_yasmin-karim@DFCI.Harvard.edu]
Johanna Wirtz [undefined [johanna.wirtz@uni-ulm.de]

Conflict of Interest Statement for All Authors:
There is no conflict of interest.

polymer components loaded with anti-CD40 agonist. Tumor volumes of both treated and untreated tumors were measured over time, along with survival and corresponding immune cell responses.

Results: Results showed that radiation with IBM administered to the gross tumor sub-volume can effectively boost abscopal responses in both pancreatic and prostate cancers, significantly increasing survival ($P<0.0001$ and $p<0.001$, respectively). Results also showed equal or superior abscopal responses when using field sizes smaller than the gross tumor volume compared to irradiating the whole tumor volume. These results were buttressed by observation of higher infiltration of cytotoxic CD8+T-lymphocytes in the treated tumors ($p<0.0001$) and untreated tumors ($p<0.0001$) for prostate cancer. Significantly higher infiltration was also observed in treated tumors ($p<0.0001$) and untreated tumors $p<0.01$) for pancreatic cancer. Moreover, the immune responses were accompanied by a positive shift of pro-inflammatory cytokines in both prostate and pancreatic tumors.

Conclusions: The approach targeting gross tumor sub-volumes with radiation and IBM offers opportunity for boosting the abscopal effect, while significantly minimizing healthy tissue toxicity. This approach proffers a radio-immunotherapy dose-painting strategy that can be developed for overcoming current barriers of immunosuppression especially for immunologically cold tumors.

Keywords

radiotherapy; immunogenic biomaterials; abscopal effect; tumor subvolume

Introduction

Cancer is a leading cause of death world-wide, with over 18.1 million new cases a year, and 9.6 million deaths.[1] Radiotherapy (RT) is one of the main modalities for cancer treatment designed to selectively kill local tumor cells within the irradiation field. Recent developments on the abscopal effect[2] proffer a promising frontier in extending the use of RT to treatment of both localized and metastatic disease. The abscopal effect describes response to treatment by cancer cells located outside the radiation field or distant from the irradiated local tumor.[3–4] Work by Formenti, Demaria, and co-workers has connected the abscopal effect to mechanisms involving the immune system.[5–9] Over the years there has been increasing evidence that abscopal response rates are low due to widespread presence of immunosuppression at tumor sites, with only a minority of patients currently showing such responses.[10,11] These low responses are characterized by low infiltration and action of immune cells like antigen presenting cells (APCs) and $CD8^+$ T cells, especially for immunologically 'cold' tumors like prostate and pancreatic cancers.[10] The development of more effective approaches to boost abscopal response rates is needed in order to effectively leverage this approach in treatment of both local and metastatic disease.

Here we investigate an approach that employs one fraction of RT with immunogenic biomaterials (IBM), which can make the tumor microenvironment more immunogenic, with significant infiltration of immune cell populations needed for effective abscopal responses. Recent research in the vaccine and immunotherapy fields has revealed that some polymeric biomaterials may be designed to program and control the infiltration of a variety of immune cells.[12–14] These studies reveal this activity is influenced by the physicochemical properties

of the material and that the choice of polymer weight and degradation of the polymeric components are important factors in determining this activity.[14–17] Here we employ IBM with immunogenic polymer components PLGA (poly-lactic-co-glycolic acid) and alginate, which have been shown to significantly enhance immunogenicity[12–14] and infiltration or maturation of APCs,[15–17] which are crucial for boosting the abscopal effect.[5,8] The IBM further strategically incorporates a component of agonistic anti-CD40 whose sustained presence[5,18,19] within the tumor microenvironment can serve as a local base for sustainably supporting the activity of infiltrating CD40+APCs in boosting tumor specific cytotoxic T cell's action.[5,19–21] A particular focus here is investigating such action for poorly immunogenic tumors[22–24], including prostate tumors, which do not express CD40.[23,24] The customizable IBM further allows for incorporation of theranostic nanoparticles which can provide contrast for image-guided RT,[19] with potential to replace biomaterials like fiducial markers[25] currently used during radiotherapy, at no additional inconvenience to patients.[20, 21]

While RT itself can be a pro-immunogenic modifier of the tumor microenvironment,[2, 26–28] we investigate the use of one RT fraction as a strategy to minimize immunosuppressive effects of RT, especially on infiltrating immune-cell populations such as peripheral APCs or CD8+ cytotoxic T cells post RT. These immune cells are particularly radiosensitive[29] and so repeated fractions of RT are likely to suppress their action needed to generate a robust abscopal effect.[29,30] Also, studies have shown that RT with large field sizes can be immunosuppressive, which would hamper the generation of a robust immune-mediated abscopal responses.[29,30] In this respect, we carried out further studies with varying field sizes,[31] including field sizes smaller than the gross tumor volume sub-volume (GTV/SV).

Materials and methods

Cell lines and cell culture materials

To generate prostate tumors, C57BL/6 background TRAMP-C1 cancer cells were purchased from American Type Culture Collection (ATCC, Manassas, VA). In addition to generate castration-resistant prostate cancer cells, androgen deprived TRAMP-C1 (AD-TRAMP-C1) cells were generated by culturing TRAMP-C1 cells for 14 days in androgen-deprived medium (Dulbecco's Modified Eagle's Medium (DMEM) (GIBCO) with10 nM flutamide and 10% dextran-coated charcoal-treated FBS) and maintained in the same culture media as shown in previous studies.[32] For pancreatic cancer, C57BL/6 background Panc-02 cells were obtained from the National Cancer Institute. The cells were cultured in DMEM (GIBCO) with 10% FBS (Sigma) and 1% penicillin/streptomycin (Invitrogen). All cells were grown in a humified incubator at 37 °C under 5% CO_2 atmosphere. All experiments were performed using cells passage number less than 30 and all injected cells were tested to be mycobacterium-free to avoid any potential adjuvant effect.

Immunogenic Biomaterials (IBM)

IBM were developed with biocompatible polymer components that have been shown to enhance immunogenicity including PLGA (poly-lactic-co-glycolic acid) (M.W.:50–50 kDa) and sodium alginate (ALG) nanoparticle components which were obtained with

acetone from Sigma-Aldrich. Twenty μg of monoclonal anti-mouse CD40 (FGK4.5/FGK45) antibody (BioXcell) was used as immunoadjuvant for each payload. Three hundred mg of polymer components was added to 3.5 mL of acetone and mixed into a homogenous solution. The Harvard apparatus (Harvard Bioscience, Holliston, MA, USA), was used to infuse the solution into the silicon tubing (ID:1/32″) (Saint-Gobain Performance Plastics Laboratory Division, USA) at a constant flow for shaping the IBM. The colloid was cured under 50°C for 48 hours. After curing, the silicon tubing was cut into fiducial marker lengths 3–5 mm as appropriate and extracted and loaded with 20 ug of immunoadjuvant payload. Brachytherapy 18 gauze needles (IZI Medical Products) were used to administered IBM intratumorally as performed clinically for fiducials using one IBM insertion per tumor under isoflurane anesthesia.

Mice

Eight- to twelve-weeks-old healthy C57BL/6 background wild ($W^{+/+}$) male and female mice were purchased from Taconic mice (C57BL/6NTac), Hudson, New York, USA and Jackson lab (C57BL/6J), Bar Harbor, Main, USA and maintained under pathogen-free conditions in the animal facility at Dana Farber Cancer Institute (DFCI) Boston,Massachusetts, USA. Mice were held in groups of five in standard cages under a 12 hours light/dark cycle, with access to food and water ad libitum. All animal procedures were conducted according to the protocols approved by Institutional Animal Care and Use Committee (IACUC) in compliance to the guidelines and regulations for the proper use and care of laboratory rodents (DFCI IACUC-15-040 and -17-010).

Subcutaneous tumors

To generate subcutaneous (SQ) prostate tumors, TRAMP-C1 cells (1×10^6 cells/tumor) were injected subcutaneously in the contralateral flanks of the male mice. For SQ model of castration resistant prostate cancers androgen deprived, AD-TRAMP-C1, cells (5×10^5 cells/tumor) were injected subcutaneously in contralateral flanks of the male mice (the term AD-Prostate cancer has been used throughout the manuscript). For pancreatic cancers, Panc-02 cells (1.5×10^5 cells/tumor) were injected SQ in both flanks of the male or female mice. In all cases, cancer cells were suspended in PBS and insulin syringes with 18 to 22-gauge size needle were used for tumor cell injection. Animals were observed minimum two times a week after cell implantation to monitor tumor growth. All mice were maintained, and the study was conducted following the IACUC-approved protocol (DFCI IACUC-15-040).

Orthotopic tumors

Orthotopic *in-vivo* syngeneic prostate mouse tumors were also generated in male mice (Taconic mice) by injecting 2.5×10^5 cells suspended in matrigel with high concentration (HC) of growth factors (Corning) in a 1:1 ratio to the right anterior prostate following standard protocol.[33] After closing the abdominal wall, one SQ tumor was implanted on the opposite flank in all of these mice under the same anesthesia. Survival assays were performed to monitor the post-treatment length of survival duration. All mice were maintained in the DFCI Animal Core Facility following intuitional IACUC approved protocol (DFCI IACUC-17-010). Details in supplementary section.

Experimental design

Mice which developed two tumors around 14 days post-implant were selected to be included in the study. When the tumor reached 3–5 mm in diameter, treatable mice were randomized and divided into groups according to each study design. Each study was matched with gender and age. Mice were also observed at least twice weekly to assess their physical conditions. In all studies, tumor measurements and body weight were measured at least twice a week and mice survival was monitored, to observe the efficacy of the treatments. The sizes of both treated and untreated tumors on each animal were monitored and the tumor growth plotted over time. Tumor diameters were monitored manually by a digital Vernier caliper. The volume was calculated using the formula: Tumor Volume = $[1/2 *L*(W^2)]$ where L and W are the length and width of the tumor, respectively. The length was measured along the imaginary longitude of the leg and the width was measured in the direction of the latitude. For orthotopic tumors, treatments were given directly to one of the SQ tumor and survival study was performed to monitor the outcome of the treatment. All animal experiments were conducted in compliance with the guidelines and regulations set by the institutional IACUC.

Small animal image-guided radiotherapy and CT imaging

A small animal radiation research platform (SARRP, Xtrahl, Inc., Suwanee, GA, USA) at the DFCI animal facility was used for image-guided radiotherapy using 220 kVp, 13 mA, and 0.15 mm copper (Cu) filter at 2–10 Gy. CT image of the animals were performed with 65 kVp and 0.8 mA. The CT images were used for a single fraction image-guided radiotherapy to one of the implanted SQ tumor (treated). For studies comparing different field sizes, 10×10 or 5×5 mm^2 collimators were used for irradiations of the volumes larger than the gross tumor volume, as the planning treatment volume (PTV) and clinical treatment volume (CTV) referred to this manuscript as PTV/CTV. Meanwhile, 3×3 mm^2 collimator was used for irradiating only a sub-volume (SV) of a gross tumor volume (GTV), referred to here as the GTV/SV. Mice were anesthetized with isoflurane during CT imaging and radiation.

Statistical Analysis

Statistical analysis results are presented as mean ± SEM. Statistical analysis were carried out using GraphPad Prism 8.0 statistical software (GraphPad Software Inc.). Survival data were plotted using GraphPad Prism 8.0. Log-rank (Mantel-Cox) and Gehan-Breslow-Wilcoxon tests were employed to determine the significance of the Kaplan–Meier survival analysis. A p-value <0.05 was considered significant with 95% or higher level of confidence interval (*p<0.05, **p< 0.01, ***p< 0.001, and ****p< 0.0001).

(Methods and materials section is continued in the supplementary file.)

Results and discussion

The modus operandi for the IBM approach to boost abscopal response rates is illustrated in Fig.1A. RT inflicts damage to tumor cells, generating tumor associated neoantigens which can be taken up by antigen presenting cells (APCs). The IBM administered into the

treated tumor enables sustained recruitment and activation of the APCs as the immunogenic polymer components of the IBM biodegrade to boost *in-situ* vaccination. The APCs can then travel to the lymph nodes to induce T-cell activation, and ultimate clonal expansion of $CD8^+$ cytotoxic T cells recognizing the tumor-specific antigens. Activated cytotoxic T-cells directed against the tumor-specific antigens then infiltrate the treated tumor as well as untreated tumors. The infiltrating cytotoxic T-cells then kill tumor-cells, resulting in additional tumor-associated antigens being released and ensuing expansion of effector T cell clones against additional antigenic targets, effectively establishing the cancer immunity cycle.[24–26]

Figure 1 demonstrates the overall strategy of this research work. C57BL/6 background syngeneic animal models of prostate and pancreatic cancers were implanted with two contralateral tumors in each mouse (details in the method section), Mice which developed two tumors were randomized and treated with IBM and/or one fraction of image-guided radiotherapy (IGRT) to one of the implanted SQ tumors. IGRT was performed using SARRP (Fig. 1B), where different sized collimators were used to deliver IGRT in different target volumes (Fig. 1C–D).

To investigate the potential to spare normal healthy tissue, IGRT of different field sizes was performed (Fig. 2 A–B, and Supplementary Fig 1A–B) to compare the surrounding tissue damage. Results for larger field sizes, that encompass the planning or clinical target volume (PTV/CTV), versus smaller field sizes targeting a sub-volume of the gross tumor volume (GTV/SV) were analyzed for ɣH2Ax to observe double strand DNA breakage. Results quantifying ɣH2Ax corroborate the potential for substantial reduction of radiation toxicity in normal tissue surrounding the tumor. A significantly smaller area of damaged tissue was identified by immunofluorescence staining of the DNA damage response repair histone ɣH2Ax when using 3×3 mm^2 radiotherapy field size which is smaller than the tumor size ($>4\times4$ mm^2) (Fig. 2C–D and supplementary Fig. 2A and B).

Starting with prostate cancer model, animals with tumors generated from TRAMP-C1 (Prostate cancer) and AD-TRAMP-C1 (castration resistant prostate cancer/AD-prostate cancer) cells were investigated. Fig. 3A illustrates the IBM and the treatment design used for this purpose. Based on the prior research in pancreatic cancer,[26] 5Gy of RT (^{5GY}RT) was administered to one of the implanted two SQ tumor with or without the treatment of IBM in the prostate cancer model (TRAMP-C1). The highest reduction of tumor volume was observed with the combination treatment of 5Gy+IBM (^{5Gy}RT+IBM) in both treated ($p<0.001$) and untreated (abscopal, $p<0.01$) tumors compare to the RT cohort (Fig. 3B and Supplementary Fig. 3A). Additionally, a survival study in the same tumor type showed significant increase in survival percent and survival duration with this combination treatment (^{5Gy}RT+IBM, $p<0.001$) compared to RT (Fig. 3C). In both cases 5 Gy of RT was given as a single dose. Further analysis was performed in castration resistant prostate cancer model (AD-prostate cancer) using this combination treatment (RT +IBM), where RT dose was titrated from 2 to 10 Gy. Here, 5 Gy of RT+IBM (^{5Gy}RT+IBM) also resulted in most significant abscopal response rate ($p<0.01$) compared to other RT doses (Fig. 3D), without any significant change in the body weight and body score of the treated mice (Supplementary Fig. 3B). Additional results showed a significant increase in survival rate

($p< 0.0001$) with ^{5Gy}RT+IBM and consistently resulted in long term survivors (Fig. 3E) in this aggressive AD-prostate cancer model. The highest infiltration of APCs (dendritic cells) on day 7 post treatment was also observed for ^{5Gy}RT+IBM treatment cohorts for the treated AD-prostate cancers ($p<0.001$) (Fig. 3F) corresponding to the results for the highest abscopal response. These results suggest that higher RT doses are not necessarily more effective in achieving an abscopal effect with IBM.

Further investigation was performed in castration resistant/AD-prostate cancers to evaluate the response for this combination treatment, ^{5Gy}RT+IBM, comparing variation of the field sizes for treatment volume, PTV/CTV vs. GTV/SV (Fig. 4A). Both the field sizes showed significant increase in abscopal response rates ($p<0.01$ for PTV/CTV and $p<0.001$ for GTV/SV) in a SQ model with no significant difference between the field sizes (Fig.4B and Supplementary Fig. 4A). Increase in survival rate was also observed for treatment in both field sizes ($p<0.001$ for GTV/SV to $p<0.01$ for PTV/CTV) in an orthotopic model with higher survival duration with the group treated with the smaller field size (GTV/SV) (Fig. 4C). Furthermore, the treated (SQ) tumors also showed significant intratumor infiltration of APCs ($p<0.0001$ and $p<0.0001$ for PTV/CTV and GTV/SV) (Fig. 4D and Supplementary Fig. 4B) when analyzed on day 7 post-treatment. Meanwhile a corresponding increase in T cells infiltration was also observed in both treated (SQ) and untreated (orthotopic) AD-Prostate tumors with no significant difference for the combination treatment with different field sizes (Fig. 4E and supplementary Fig. 4C). Altogether, the data suggests that radiotherapy with IBM, even for field sizes smaller than the tumor sub-volume, can still significantly boost abscopal response rates in prostate cancer treatment.

To obtain additional insights in the abscopal response, an ELISA analysis was performed for inflammatory cytokines on collected serum on post treated day 12 from AD-Prostate cancer orthotopic model. Increased of $CD8^+$ T-cells and anti-tumor activity of APCs induces higher pro-inflammatory cytokines to perform the tumoricidal effect[33,34]. Pro-inflammatory cytokines, including IL-2,[34] IL-12,[33–35] have been well characterized as associated with anti-tumor responses. An overall significant shift towards anti-tumor/pro-inflammatory cytokines including IL-2 and IL-12 was observed with the ^{5Gy}RT+ IBM treatment with no significant difference for field sizes, PTV/CTV ($p<0.01$) and GTV/SV ($p<0.01$) (Fig. 4F and Supplementary Table1), which is consistent with the observations in figures 4A–E.

For pancreatic cancer model where contralateral SQ tumors were generated from Panc-02 cells, combination treatment (^{5Gy}RT+IBM) also showed a major boost in abscopal responses ($p<0.0001$ and $p<0.0001$ compared with RT and IBM, respectively) similar to observations made with both type of prostate tumors (Fig. 5A–B). Furthermore, ^{5Gy}RT+IBM showed no significant difference in combination treatment with field size variation ($p<0.001$ and $p<0.001$ for PTV/CTV and GTV/SV field sizes, respectively) (Fig. 5C and Supplementary Fig. 5A). Significant increase in survival rate was also observed for both field sizes ($p<0.01$, PTV/CTV and $p<0.001$, GTV/SV), albeit higher survival duration for the smaller field size (Fig. 5D). *Ex-vivo* analysis of the tumor tissue on day-7 post-treatment consistently showed significant enhancement of the $CD8^+$ cytotoxic T cell infiltration in both treated (Supplementary Fig. 5B) and untreated (Fig. 5E and) tumors with ^{5Gy}RT+IBM treatment, PTV/CTV ($p<0.001$) and GTV/SV ($p<0.01$) compared to control. No significant difference

was shown for different field sizes. Similar to prostate cancers, serum collected from *ex-vivo* pancreatic cancer animals also showed a significant high anti-tumor/pro-inflammatory cytokine surge in the combination treatment cohorts with no significant difference when different field sizes were investigated (Fig. 5F, and Supplementary Table1).

Overall, the results from the different investigations in different tumor types consistently indicate that radiotherapy with IBM, even with tumor sub-volume field sizes can be an effective therapeutic strategy for boosting the abscopal effect. This radio-immunotherapy approach has a number of potential advantages. First, it has the potential for major sparing of healthy tissue when targeting the gross tumor sub-volume with smaller field sizes and IBM to create an immunogenic hub. The addition of margins during RT treatment planning is a time-consuming and error-prone step, often resulting in the irradiation of more normal tissue. The development of such an approach, which can afford the killing of tumor cells outside the radiation field via the abscopal effect, would make the addition of margins like the clinical target volume (CTV) obsolete for this type of tumors, with major sparing of normal healthy tissue. This would be particularly important for subjects who may not otherwise qualify for radiotherapy because they have reached their normal tissue toxicity limits during prior treatment.[38]

Another important aspect of this approach is the use of just one fraction of radiotherapy in generating neoantigens and exposing tumor associated antigens. This may further reduce the surrounding tissue toxicity[38,39] and immunosuppressive effect of radiotherapy.[9,10] This is valuable, since the infiltrating immune cell populations that are crucial for boosting the abscopal effect (such as APCs or $CD8^+$ cytotoxic T cells) are particularly radiosensitive.[10, 38] High radiation dose or repeated fractions of RT are likely to suppress or stifle their action needed to generate a robust abscopal effect.[38]

The ‘positive’ shift of the cytokines towards pro-inflammatory/anti-cancer mode[34] observed in this study support overall effectiveness of the treatment strategy. IL-2, which has been one of the most researched cytokine for enhancing potent antitumor activity against many cancers,[34,35] showed an increase in both prostate and pancreatic tumor micro-environments. This cytokine has been shown to play a critical role in differentiation of CD4+ T cells into a variety of subsets, and promotion of CD8+ T-cell and other cytotoxic activity.[34–36] IL-12, is another well characterized potent inducer of antitumor immunity, mainly produced by pro-inflammatory APCs, like dendritic cells, monocytes, and B cells.[36,37] Here, we observed increased infiltration of APCs in the tumor microenvironments treated with ^{5Gy}RT+IBM, consistent with increase in IL-12 secretion (Fig. 4F, 5F and Supplementary Table1), which supports promotion of antitumor activity. Altogether, the increased infiltration of immune cells like APCs and $CD8^+$ T-cells, as well as the induction of anti-tumor cytokines like IL-2 and IL12 reflect the same anti-tumor immune surge towords the abscopal effect. These findings provide the basis for additional research towards further optimizing the treatment parameters of this approach to substantially boost the abscopal response rates with increased sparing of healthy tissue.

The approach investigated here is promising in that it can be developed to boost high abscopal response rates particularly for immunologically cold tumors like pancreatic

cancer, which is often diagnosed at metastatic stage, as well as metastatic castration resistant prostate cancers. For these cancers, current curative treatment options are limited and prognosis is extremely poor.[23–25] The use of IBM to make the tumor microenvironment more immunogenic, provides opportunities for administering the IBM to immunosuppressive tumor sub-volumes e.g. hypoxic volumes. Such volumes can be identified via functional imaging using magnetic resonance imaging (MRI).

Conclusion

Altogether, the approach targeting tumor sub-volumes with RT and IBM offers an opportunity for boosting the abscopal effect, while significantly minimizing normal tissue toxicity. The results provide significant impetus for further studies to develop this approach and optimize treatment parameters including for other tumor types.

Supplementary Material

Refer to Web version on PubMed Central for supplementary material.

Acknowledgements:

Special thanks to Sada N. Breegi, Clinical Veterinarian and Catherine Sypher, Manager, Technical Services, Animal Resource Facility (ARF) at Dana Farber Cancer Research Institute/A Teaching Affiliate of Harvard Medical School, Boston, Massachusetts for technical support.

Funding Statement:

National Cancer Institute of the National Institutes of Health under Award Numbers R01CA239042 and R21CA205094-01A1. The content is solely the responsibility of the authors and does not necessarily represent the official views of the National Institutes of Health.

Data Availability Statement for this Work:

Research data will be shared upon request to the corresponding author.

References

1. Bray F, Ferlay J, Soerjomataram I, Siegel RL, Torre LA, Jemal A. Global cancer statistics 2018: GLOBOCAN estimates of incidence and mortality worldwide for 36 cancers in 185 countries [published correction appears in CA Cancer J Clin. 2020 Jul;70(4):313]. CA Cancer J Clin. 2018;68(6):394–424. doi:10.3322/caac.21492 [PubMed: 30207593]
2. MOLE RH. Whole body irradiation; radiobiology or medicine?. Br J Radiol. 1953;26(305):234–241. doi:10.1259/0007-1285-26-305-234 [PubMed: 13042090]
3. Hu ZI, McArthur HL, Ho AY. The Abscopal Effect of Radiation Therapy: What Is It and How Can We Use It in Breast Cancer?. Curr Breast Cancer Rep. 2017;9(1):45–51. doi:10.1007/s12609-017-0234-y [PubMed: 28344743]
4. Siva S, MacManus MP, Martin RF, Martin OA. Abscopal effects of radiation therapy: a clinical review for the radiobiologist. Cancer Lett. 2015;356(1):82–90. doi:10.1016/j.canlet.2013.09.018 [PubMed: 24125863]
5. Ngwa W, Irabor OC, Schoenfeld JD, Hesser J, Demaria S, Formenti SC. Using immunotherapy to boost the abscopal effect. Nat Rev Cancer 2018;18:313–322. [PubMed: 29449659]
6. Stamell EF, Wolchok JD, Gnjatic S, Lee NY, Brownell I. The abscopal effect associated with a systemic anti-melanoma immune response. Int J Radiat Oncol Biol Phys. 2013;85(2):293–295. doi:10.1016/j.ijrobp.2012.03.017 [PubMed: 22560555]

7. Demaria S, Coleman CN, Formenti SC. Radiotherapy: Changing the Game in Immunotherapy. Trends Cancer. 2016;2(6):286–294. doi:10.1016/j.trecan.2016.05.002 [PubMed: 27774519]
8. Demaria S, Ng B, Devitt ML, et al. Ionizing radiation inhibition of distant untreated tumors (abscopal effect) is immune mediated. Int J Radiat Oncol Biol Phys. 2004;58(3):862–870. doi:10.1016/j.ijrobp.2003.09.012 [PubMed: 14967443]
9. Johnson CB, Jagsi R. The Promise of the Abscopal Effect and the Future of Trials Combining Immunotherapy and Radiation Therapy. Int J Radiat Oncol Biol Phys. 2016;95(4):1254–1256. doi:10.1016/j.ijrobp.2016.02.067 [PubMed: 27354132]
10. Bonaventura P, Shekarian T, Alcazer V, et al. Cold Tumors: A Therapeutic Challenge for Immunotherapy. Front Immunol. 2019;10:168. Published 2019 Feb 8. doi:10.3389/fimmu.2019.00168 [PubMed: 30800125]
11. Ochoa de Olza M, Navarro Rodrigo B, Zimmermann S, Coukos G. Turning up the heat on non-immunoreactive tumours: opportunities for clinical development. Lancet Oncol. 2020;21(9):e419–e430. doi:10.1016/S1470-2045(20)30234-5 [PubMed: 32888471]
12. Wang H, Mooney DJ. Biomaterial-assisted targeted modulation of immune cells in cancer treatment. Nat Mater. 2018;17(9):761–772. doi:10.1038/s41563-018-0147-9 [PubMed: 30104668]
13. Ali OA, Emerich D, Dranoff G, Mooney DJ. In situ regulation of DC subsets and T cells mediates tumor regression in mice. Sci Transl Med. 2009;1(8):8ra19. doi:10.1126/scitranslmed.3000359
14. Szekalska M, Puciłowska A, Szymańska E, Ciosek P & Winnicka K Alginate: Current Use and Future Perspectives in Pharmaceutical and Biomedical Applications. Int. J. Polym. Sci. 2016, 1(17).
15. Park J, Babensee JE. Differential functional effects of biomaterials on dendritic cell maturation. Acta Biomater. 2012;8(10):3606–3617. doi:10.1016/j.actbio.2012.06.006 [PubMed: 22705044]
16. Babensee JE, Paranjpe A. Differential levels of dendritic cell maturation on different biomaterials used in combination products. J Biomed Mater Res A. 2005;74(4):503–510. doi:10.1002/jbm.a.30429 [PubMed: 16158496]
17. Andorko JI, Jewell CM. Designing biomaterials with immunomodulatory properties for tissue engineering and regenerative medicine. Bioeng Transl Med. 2017;2(2):139–155. Published 2017 May 16. doi:10.1002/btm2.10063 [PubMed: 28932817]
18. Mueller R, Moreau M, Yasmin-Karim S, et al. Imaging and characterization of sustained gadolinium nanoparticle release from next generation radiotherapy biomaterial. Nanomaterials (Basel) 2020;10:2249
19. Ngwa W, Kumar R, Moreau M, Dabney R, Herman A. Nanoparticle drones to target lung cancer with radiosensitizers and cannabinoids. Front Oncol 2017;7:208 [PubMed: 28971063]
20. Ngwa W, Boateng F, Kumar R, et al. Smart radiation therapy biomaterials. Int J Radiat Oncol Biol Phys 2017;97:624–637. [PubMed: 28126309]
21. Moreau M, Yasmin-Karim S, Kunjachan S, et al. Priming the abscopal effect using multifunctional smart radiotherapy biomaterials loaded with immunoadjuvants. Front Oncol 2018;8:56 [PubMed: 29594038]
22. Wu J, Cai J. Dilemma and Challenge of Immunotherapy for Pancreatic Cancer. Dig Dis Sci. 2020 Mar 5. doi: 10.1007/s10620-020-06183-9. Epub ahead of print.
23. Moghaddami M, Cohen P, Stapleton AM, Brown MP. CD40 is not detected on human prostate cancer cells by immunohistologic techniques. Urology. 2001 Mar;57(3):573–8. doi: 10.1016/s0090-4295(00)01005-0. [PubMed: 11248650]
24. Palmer DH, Hussain SA, Ganesan R, et al. CD40 expression in prostate cancer: a potential diagnostic and therapeutic molecule. Oncol Rep. 2004;12(4):679–682. doi:10.3892/or.12.4.679 [PubMed: 15375484]
25. Keall PJ et al. The management of respiratory motion in radiation oncology report of AAPM Task Group 76. Medical Physics (2006) doi:10.1118/1.2349696.
26. Yasmin-Karim S, Bruck PT, Moreau M, et al. Radiation and local anti-CD40 generate an effective in situ vaccine in preclinical models of pancreatic cancer. Front Immunol 2018;9:2030. [PubMed: 30245691]

27. Formenti SC, Demaria S. Radiation therapy to convert the tumor into an in situ vaccine. Int J Radiat Oncol Biol Phys. 2012;84(4):879–880. doi:10.1016/j.ijrobp.2012.06.020 [PubMed: 23078897]
28. Rodriguez-Ruiz ME, Vitale I, Harrington KJ, Melero I, Galluzzi L. Immunological impact of cell death signaling driven by radiation on the tumor microenvironment. Nat Immunol. 2020;21(2):120–134. doi:10.1038/s41590-019-0561-4 [PubMed: 31873291]
29. Merrick A, Errington F, Milward K, et al. Immunosuppressive effects of radiation on human dendritic cells: reduced IL-12 production on activation and impairment of naive T-cell priming. Br J Cancer. 2005;92(8):1450–1458. doi:10.1038/sj.bjc.6602518 [PubMed: 15812550]
30. Wennerberg E, Lhuillier C, Vanpouille-Box C, et al. Barriers to Radiation-Induced *In Situ* Tumor Vaccination. Front Immunol. 2017;8:229. Published 2017 Mar 13. doi:10.3389/fimmu.2017.00229 [PubMed: 28348554]
31. Cormack RA, Sridhar S, Suh WW, D'Amico AV, Makrigiorgos GM. Biological in situ dose painting for image-guided radiation therapy using drug-loaded implantable devices. Int J Radiat Oncol Biol Phys 2010;76:615–623 [PubMed: 19879699]
32. Wu C-T, Chen W-C, Chen M-F. The Response of Prostate Cancer to Androgen Deprivation and Irradiation Due to Immune Modulation. Cancers. 2019; 11(1):20. 10.3390/cancers11010020
33. Yasmin-Karim S, King MR, Messing EM, Lee YF. E-selectin ligand-1 controls circulating prostate cancer cell rolling/adhesion and metastasis. Oncotarget 2014;5:12097–12110. [PubMed: 25301730]
34. Grivennikov SI, Greten FR, Karin M. Immunity, inflammation, and cancer. Cell. 2010;140(6):883–899. doi:10.1016/j.cell.2010.01.025 [PubMed: 20303878]
35. Weiss JM, Back TC, Scarzello AJ, et al. Successful immunotherapy with IL-2/anti-CD40 induces the chemokine-mediated mitigation of an immunosuppressive tumor microenvironment. Proc Natl Acad Sci U S A. 2009;106(46):19455–19460. doi:10.1073/pnas.0909474106 [PubMed: 19892741]
36. Tugues S, Burkhard SH, Ohs I, et al. New insights into IL-12-mediated tumor suppression. Cell Death Differ. 2015;22(2):237–246. doi:10.1038/cdd.2014.134 [PubMed: 25190142]
37. Sheikhpour E, Noorbakhsh P, Foroughi E, Farahnak S, Nasiri R, Neamatzadeh H. A Survey on the Role of Interleukin-10 in Breast Cancer: A Narrative. Rep Biochem Mol Biol. 2018;7(1):30–37. [PubMed: 30324115]
38. Ghadjar P, Hayoz S, Bernhard J, et al. Impact of dose intensified salvage radiation therapy on urinary continence recovery after radical prostatectomy: Results of the randomized trial SAKK 09/10. Radiother Oncol. 2018;126(2):257–262. doi:10.1016/j.radonc.2017.10.025 [PubMed: 29103826]
39. van Oorschot B, Hovingh SE, Moerland PD, et al. Reduced activity of double-strand break repair genes in prostate cancer patients with late normal tissue radiation toxicity. Int J Radiat Oncol Biol Phys. 2014;88(3):664–670. doi:10.1016/j.ijrobp.2013.11.219 [PubMed: 24411188]

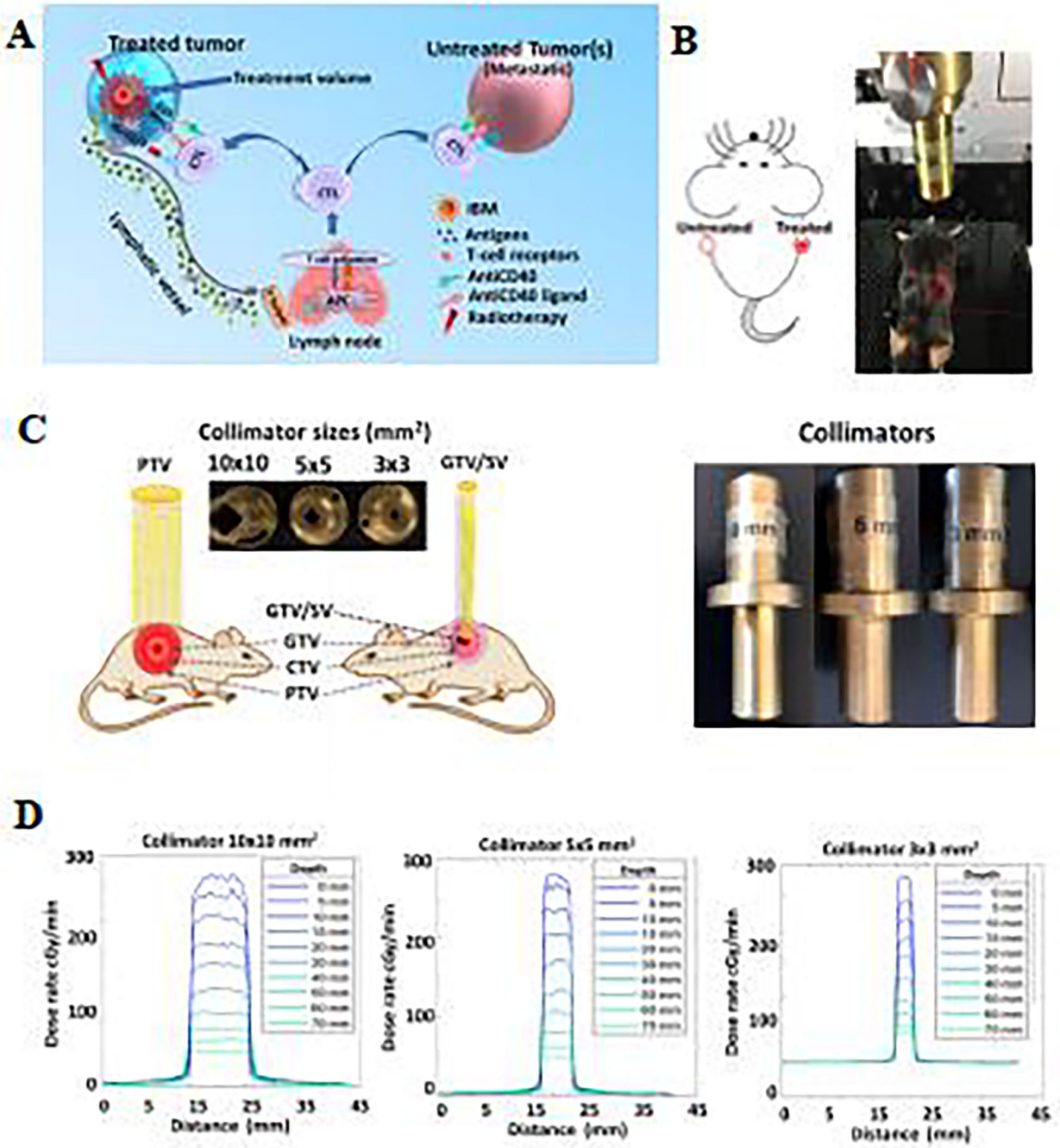

Fig. 1.

Approach to boost abscopal response rates using immunogenic biomaterials (IBM) with sub-volume radiotherapy (RT). (A) Schematic illustration of the approach to boost abscopal response rates by targeting the tumor sub-volume with image-guided radiotherapy and immunogenic biomaterials (IBM) leveraging the abscopal effect. The IBM enhances infiltration and activation of antigen presenting cells (APCs). APCs in the tumor take-up these antigens created by RT induced tumor cell damage, and travel to the lymph nodes for cross-presentation to generate tumor specific $CD8^+$ cytotoxic T lymphocytes (CTLs)

to induce anti-tumor effect.[9,23] This immune-mediated action results in high abscopal responses with regression of both treated (local), and untreated cancers, representing metastasis. (B) Targeted irradiation of one of the two implanted tumors, using SARRP. (C) A cartoon showing different tumor volumes that can be targeted with different field sizes using different sized collimators of the SARRP (left). Pictures of different sized collimators for different treatment volumes (right). (D) Representative field profiles for RT are shown for 10×10, 5×5, and 3×3 mm^2 sized collimators (SSD is 34 cm). SSD: source to surface distance.

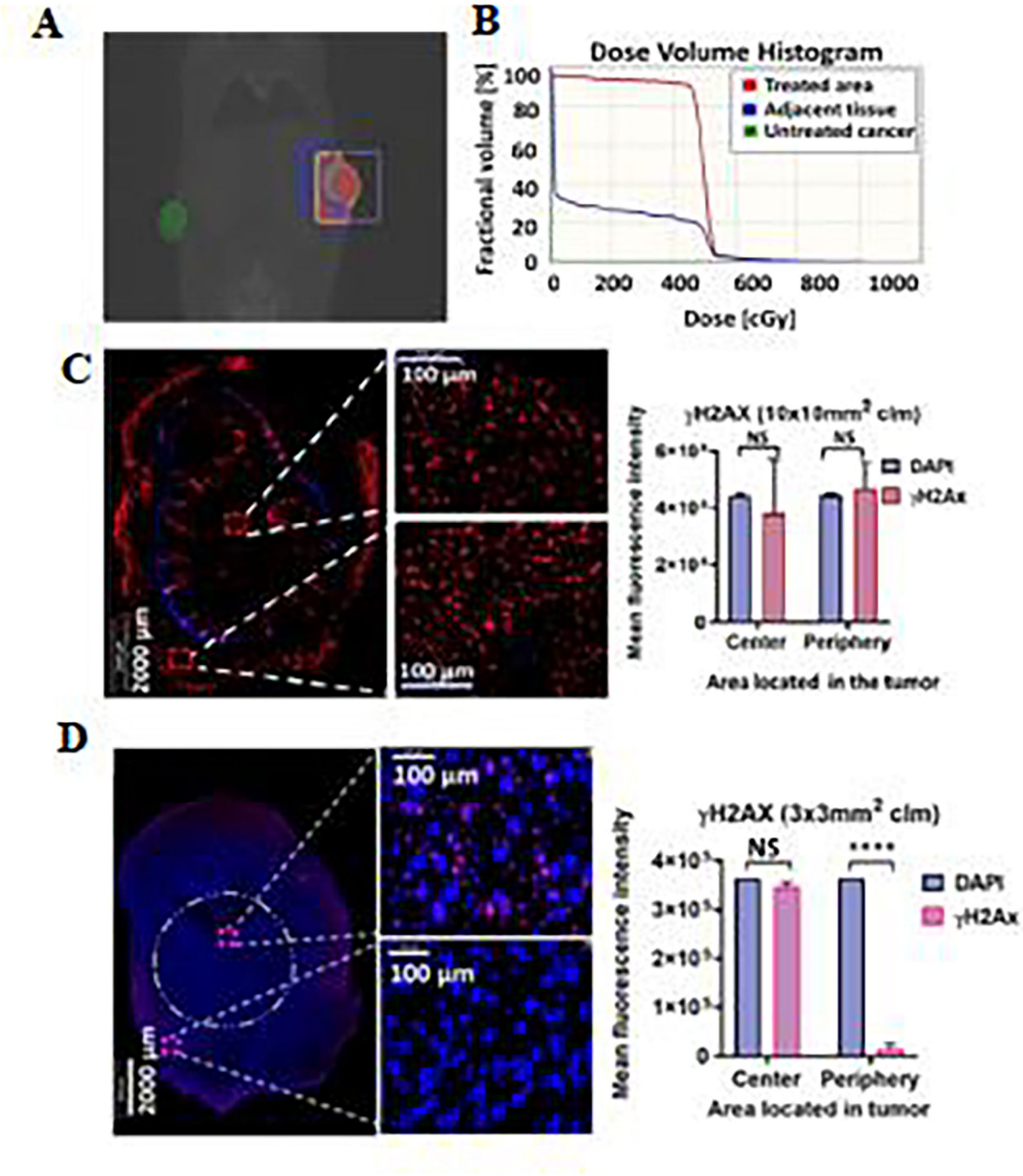

Fig. 2.

Approach to reduce normal tissue toxicity by using RT field sizes smaller than the gross tumor volume (GTV/SV). (A-B) Dose map and histogram showing irradiated regions with 10×10 mm^2 field size with direct treated area (red), adjacent tissue receiving radiation (blue), and untreated tumor receiving no radiation (green). (C) IF images and corresponding bar graphs for the DNA damage repair histone γH_2Ax (CY3, red, excitation wavelength 555 nm) and nuclei (DEPI, blue) 4 hours after IGRT to the planning target volume (PTV) with 10×10 mm^2 sized field, representing DNA damage in the center as well as in the peripheral

section of the AD-prostate tumor. (D) Similar IF image and bar graph representing DNA damage in the center (RT treated area) and relatively no damage at the peripheral section of the tumor for RT with 3×3 mm^2 sized field where only a GTV/SV of the AD-prostate tumor was irradiated. Data represents the mean +/− SD. **** $p < 0.0001$. NS: no statistical significance.

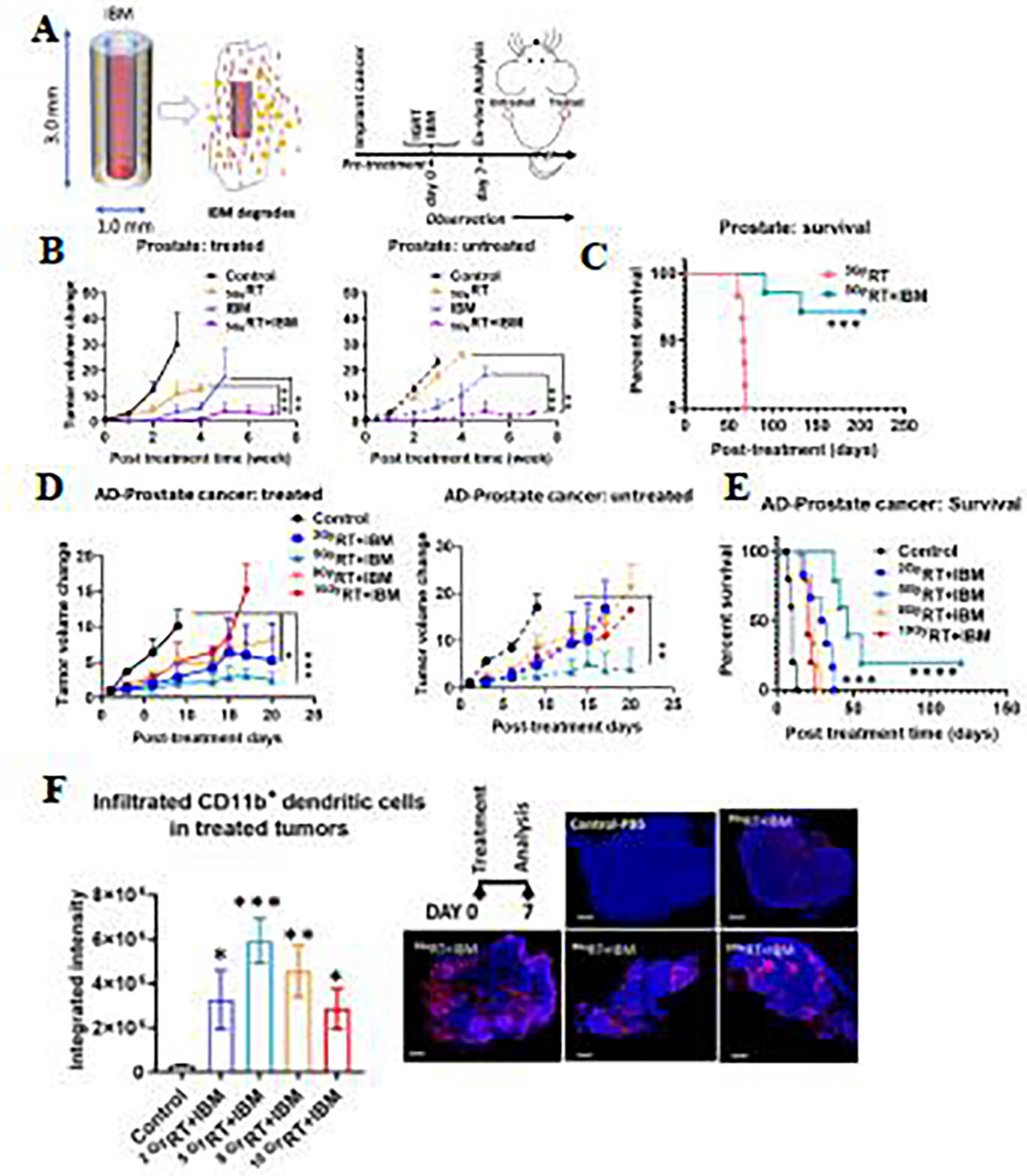

Fig. 3.

Radiation with 5 Gy of RT shows the highest abscopal response for RT+IBM. (A) Schematic diagram of IBM and study design for prostate cancer model where two tumors were implanted in contralateral flanks (SQ) and only one was treated. (B) The dynamics of the tumor volume change showing in line graphs for treated (solid line) and untreated (dashed line) prostate cancers (SQ tumors generated from TRAMP-C1 cells) where one of the two implanted SQ tumors treated with IBM, 5 Gy of RT, and in combination of ^{5GY}RT+IBM along with a control (n=5 for each cohort). (C) Kaplan-Meier survival curve of an additional

study showing percent survival of mice treated with 5 Gy (n=6) of radiotherapy versus 5 Gy of RT+IBM (n=6) for prostate cancers. (D) Line graphs showing dynamics of the tumor volume change for both treated (solid line) and untreated (dash line) tumors in AD-prostate cancer model (SQ tumors generated from AD-TRAMP-C1 cells) where a control cohort was compared with the combination treatment (RT+IBM) with variating the RT doses for 2, 5, 8, or 10 Gy (n=5). (E) Kaplan-Meier survival curve showing percent survival for the same treatment cohorts comparing with control (n=5). (F) Bar graph and representative images showing the infiltration of APCs like dendritic cells (CD11b+) to the treated tumors on day 7 post treatment for the same cohorts (comparing with control). *Ex-vivo* treated tumors were resected. Paraffin embedded 4 mm thin sections were treated with CD11b+ antibody for IF analysis. Bar graph represents the average integrated fluorescent intensity for different cohorts (n=3). CY3 (red) represents infiltrated CD11b+ dendritic cells and DAPI is for nucleus staining. Scale bar is 2,000 μm. RT was given using 10×10 mm^2 sized collimator. Data represents the mean +/− SD. ** $p< 0.01$, *** $p< 0.001$, **** $p< 0.0001$.

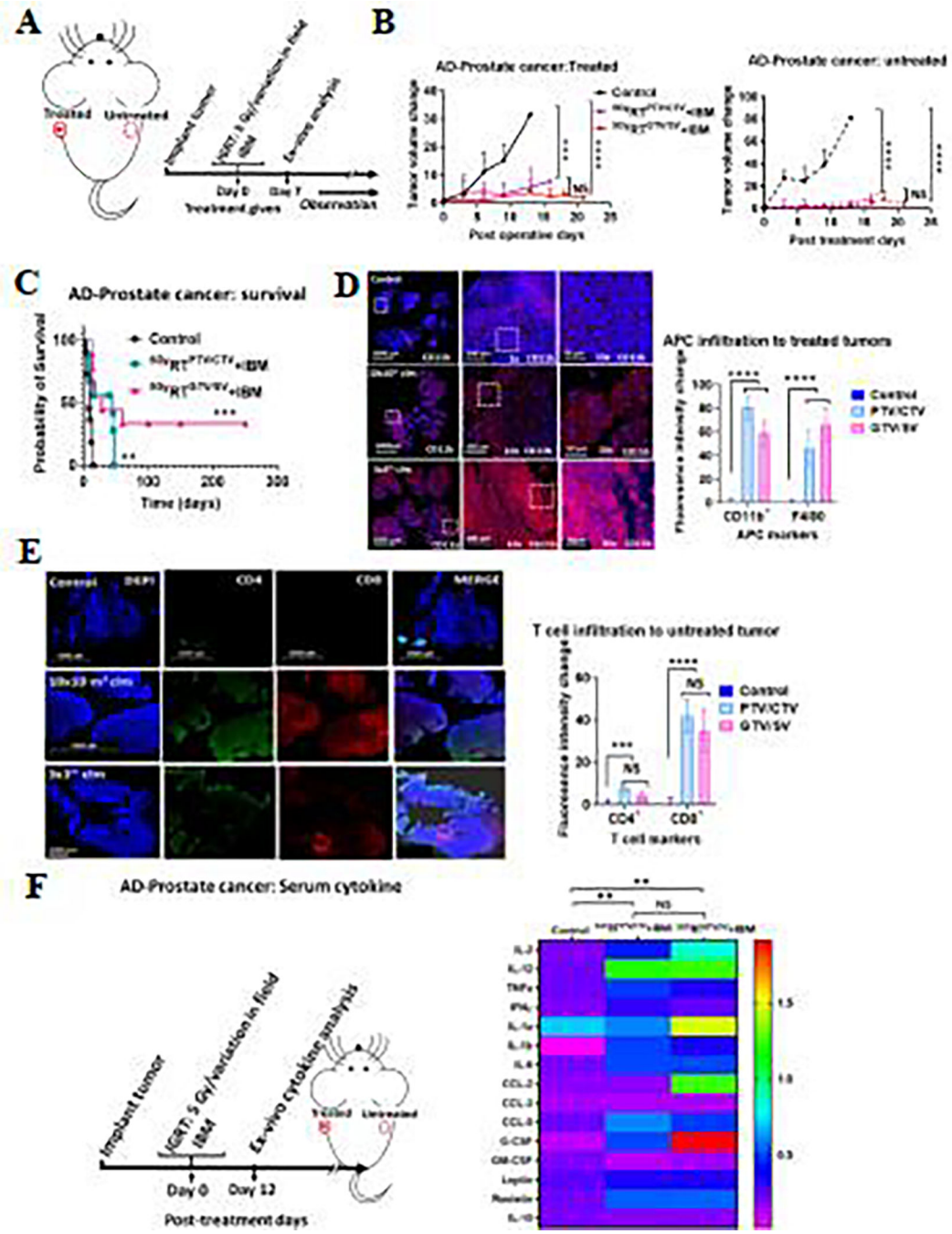

Fig. 4.

Treatment with different field sizes in a castration resistant prostate cancer/AD-prostate cancer model. (A) Treatment design. (B) Comparing tumor volume change in both treated ($p<0.001$, $p<0.0001$) and untreated ($p<0.0001$, 0.0001) AD-prostate cancers in SQ model, where 5 Gy of IGRT with IBM (^{5Gy}RT+IBM) was given in one of the implanted tumors compared with control cohorts. IGRT was delivered using 10×10 mm^2 collimators (cohort $^{5Gy}RT^{PTV/CTV}$+IBM, n=5), or 3×3 mm^2 collimators (cohort $^{5Gy}RT^{GTV/SV}$+IBM, n=5 for each cohort); Here AD-TRAMP-C1 cells were implanted subcutaneously in two

contralateral flanks. (C) A Kaplan-Meier survival curve for AD-prostate cancer orthotopic model, n=9 ($p < 0.01$ for 10×10 mm^2 and $p<0.001$ in 3×3 mm^2 field sizes for RT). (D) Representative images showing the infiltration of APCs like dendritic cells, DCs, ($CD11b^+$) to the treated tumors (SQ) on day 7 post treatment comparing different field sizes for treatment. *Ex-vivo* treated tumors were resected. Paraffin embedded 4 mm thin sections were treated with CD11b+ antibody for IF analysis. Bar graph is the quantified representation of both DCs ($p<0001$) and macrophages ($p<0.0001$) infiltration in treated tumor microenvironment. The y-axis showing the average integrated fluorescent intensity change for different cohorts (n=3). (E) Seven-day post-treatment comparison of $CD4^+$ ($p<0.001$) and $CD8^+$ ($p<0.0001$) T-cell infiltration into untreated tumors (orthotopic) shown in representative images and in a bar graph. In all cases, green color represents FITC (excitation wavelength 480 nm) for $CD4^+$ and red color represents CY3 for $CD8^+$ T lymphocyte infiltration. DAPI (blue) represents for nucleus staining of the tumor tissue. Data represents the mean +/− SD. (F) Research design and a heatmap showing the OD values (at 490 nm) of serum pro- and anti-inflammatory cytokines. Mouse Cytokine ELISA assay was performed on serum collected from mice treated with combination of RT+IBM where 5 Gy of RT was delivered in one fraction for 10×10 mm^2 or 3×3 mm^2 sized fields ($^{5Gy}RT^{PTV/CTV}$+IBM vs. $^{5Gy}RT^{GTV/SV}$+IBM respectively) to one of the tumors (treated tumor), (n=5). Day twelve post-treatment serum cytokine was analyzed using an ELISA kit pretreated with antibody against the analyzed cytokines (Signosis, Inc.). ** $p< 0.01$, *** $p< 0.001$, **** $p< 0.0001$. NS abbreviates not significant.

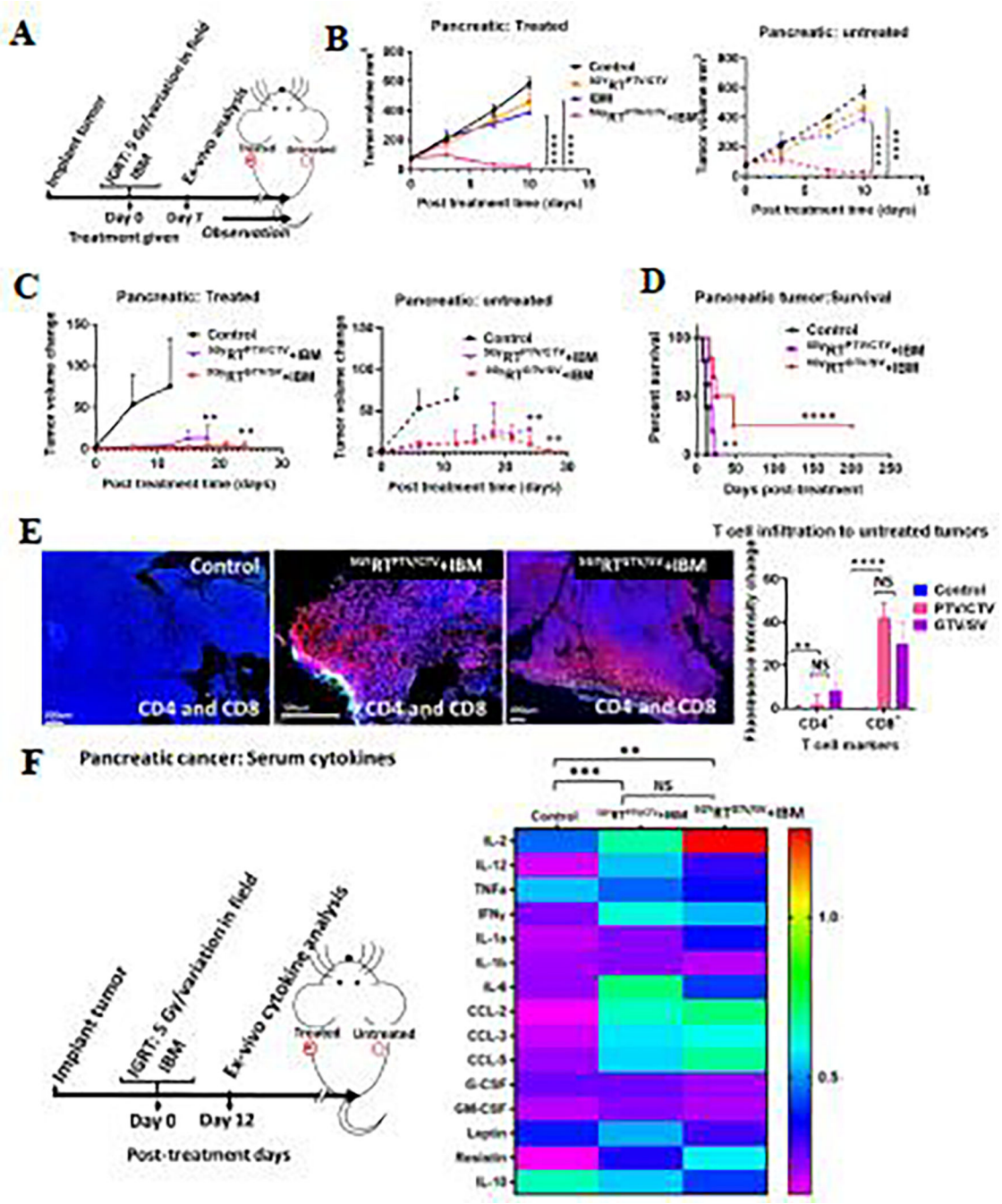

Fig. 5.

Treatment with different field sizes in pancreatic cancer. (A) Study design for pancreatic cancer model where two SQ tumors were implanted in two flanks and only one was treated with RT and/or IBM. (B) Line graphs showing real time tumor volume progression in treated (solid line) and untreated (dashed line) tumors where one of the two implanted SQ pancreatic cancers was treated with ^{5GY}RT, or IBM, or ^{5GY}RT+IBM. Control cohort was treated with PBS, (n=5, for each cohort). (C) Comparing tumor volume change with control group for both treated and untreated pancreatic cancers, where 5 Gy of IGRT and IBM

were given in one of the implanted tumors and compared with varying the field sizes for PTV/CTV ($^{5Gy}RT^{PTV/CTV}$+IBM, n=5, p<0.01 and p<0.01 for both treated and untreated cohorts respectively), or GTV/SV ($^{5Gy}RT^{GTV/SV}$+IBM, n=5, p<0.01 and p<0.01 for both treated and untreated cohorts respectively). (D) A representative Kaplan-Meier curve with p values of <0.01 and <0.0001 for PTV/CTV and GTV/SV field sizes, respectively. (E) Representative images of untreated pancreatic cancer tissue of 7-day post-treatment showing IF staining for intra-tumoral infiltration of $CD4^+$ (FITC) and CD8+ (CY5) T lymphocytes, where the tumors were treated with IBM and radiotherapy in varying field sizes ($^{5Gy}RT^{PTV/CTV}$+IBM), and $^{5Gy}RT^{GTV/SV}$+IBM). *Ex-vivo* tumors were resected and analyzed as Fig. 4. Bar graph represents the average integrated fluorescent intensity for different cohorts (n=3). FITC for infiltrated $CD4^+$ and CY5 (excitation wavelength 570 nm) represents infiltrated $CD8^+$ T cells. DAPI (blue) is for nucleus staining. Control tumors were treated with PBS. The corresponding bar graph for the fluorescence intensity change is shown in right. Data represents the mean +/− SD. (F) Heatmap for serum pro- and anti-inflammatory cytokines with control (no treatment) and in combination treatment groups with different radiation fields (n=5) for pancreatic cancers (n=5). For both cases serum was collected 12 das post treatment. ** p< 0.01, **** p< 0.0001, NS abbreviates not significant.